CFD simulations to optimize the blades design of water wheels

Drink. Water Eng. Sci., 10, 27–32, 2017
www.drink-water-eng-sci.net/10/27/2017/
doi:10.5194/dwes-10-27-2017

Drinking Water
Engineering and Science
Open Access

CFD simulations to optimize the blade design of water wheels

Emanuele Quaranta and Roberto Revelli

Department of Environment, Land and Infrastructure Engineering, Politecnico di Torino, Turin, Italy

Correspondence to: Emanuele Quaranta (emanuele.quaranta@polito.it, quarantaemanuele@yahoo.it) and Roberto Revelli (roberto.revelli@polito.it)

Received: 24 January 2017 – Discussion started: 30 January 2017
Revised: 22 April 2017 – Accepted: 24 April 2017 – Published: 16 May 2017

Abstract. At low head sites and at low discharges, water wheels can be considered among the most convenient hydropower converters to install. The aim of this work is to improve the performance of an existing breastshot water wheel by changing the blade shape using computational fluid dynamic (CFD) simulations. Three optimal profiles are investigated: the profile of the existing blades, a circular profile and an elliptical profile. The results are validated by performing experimental tests on the wheel with the existing profile. The numerical results show that the efficiency of breastshot wheels is affected by the blade profile. The average increase in efficiency using the new circular profile is about 4 % with respect to the profile of the existing blades.

1 Introduction

Electricity production on a large scale from renewable energy sources has become an important purpose in European Commission legislation. Among renewable energy sources, hydropower is the most used (Laghari et al., 2013). However, large hydropower plants require the construction of large dams, buildings and installations for the generation, regulation and transmission of power; this can cause the fragmentation of river continuity (Kallis and David, 2001). In addition, there are often many adverse effects and drawbacks in the ecosystems, for example the flooding of large areas and the interruption of river continuity. Micro-hydropower (with a net input power lower than 100 kW) is considered more ecofriendly, and payback times are generally lower than large hydropower plants. Micro-hydropower plants can also represent a strategy for decentralized and distributed micro-generation and self-sustainability, for example in irrigation networks (water utilities are significant electricity consumers, accounting for as much as 5 % of the electricity consumption of a city; Menke et al., 2016).

However, most low head and low discharge sites are still not exploited, since standard turbines cannot be economically employed under such conditions. Most of them were used in the nineteenth century as power for mills, but they are currently neglected (Bozhinova et al., 2013; Müller and Kauppert, 2004).

In Bozhinova et al. (2013), a review of hydropower converters for very low heads has been presented, and an attractive opportunity in the micro-hydro field is represented by gravity water wheels. Gravity water wheels exploit the potential energy and a portion of the kinetic energy of water. They can be classified as overshot wheels, where the water enters the wheel from the top, or breastshot water wheels, where the water fills buckets entering from the upstream side of the wheel. Breastshot water wheels can be further classified as high, middle or low, depending on whether the water entry point to the wheel is over the rotation axis (in the uppermost third of the wheel), near the axis (in the middle third of the wheel) or under the axis (in the lowest third of the wheel), respectively. In breastshot water wheels, the upstream water level can be controlled by inflow structures. When there is an overflow weir or an undershot weir (with a sluice gate to regulate the upstream water level), breastshot wheels are called slow or fast, respectively; in the latter case considering the higher flow velocity to the wheel (Quaranta and Revelli, 2016a). Low breastshot wheels for very low heads are called undershot wheels. Zuppinger and Sagebien undershot water wheels are used at sites with very low heads (typically lower

than 1.5 m) and upstream conditions that can be controlled by an inflow weir so that the approaching flow velocity is very low, generally lower than 1 m s^{-1} (Quaranta and Müller, 2017). A particular kind of fast undershot water wheel that exploits the kinetic energy of the water well is the Poncelet wheel (Poncelet, 1843). Poncelet wheels are generally installed in straight channels with no bed drops or geometric heads through the wheel. The channel drop is present downstream of the wheel, so that the blades do not interfere with the tailrace. The inflow is achieved with a sluice gate that is very close to the wheel in order to increase the flow velocity. The water jet exchanges its momentum with the wheel flowing along the blades. Water wheels that exploit the kinetic energy of flow and that can be partially immersed in water are called stream water wheels.

The maximum efficiency can be higher than 80 % for overshot water wheels (Quaranta and Revelli, 2015b), 75 % for breastshot water wheels (Quaranta and Revelli, 2015a; Quaranta and Revelli, 2016a; Vidali et al., 2016), higher than 80 % for undershot Zuppinger and Sagebien water wheels (Quaranta and Müller, 2017) and approximately 55 % for Poncelet wheels. Although water wheels are environmentally friendly (because of the large cells and low rotational speed; Müller and Kauppert, 2004; Quaranta and Müller, 2017) and efficient hydropower converters, only a small amount of research has been done on their performance characteristics in the last century. There are now some companies and research centers that are currently dealing with water wheels, especially for electricity generation.

Due to their several advantages over turbines, water wheels may constitute a suitable technology for economic development, particularly in rural areas and lower-income countries. Indeed, the efficiency can be maintained as constant over a wide range of external conditions, without acting on the pitch of the blades. The total cost of a water wheel depends on its dimensions and geometry. In Germany, overshot water wheels are currently being built (including installation and grid connection) for EUR 3900 to EUR 4340 for each kW of installed power capacity. Undershot wheels cost between EUR 6900 and EUR 8670 for each kW and Archimedes screws cost approximately EUR 7380 to EUR 7804 for each kW. For comparison, low head Kaplan turbines cost from EUR 13 000 to EUR 13 900 kW. Water wheels cost between 33 and 66 % of the equivalent prices for turbines (Müller and Kauppert, 2002). Payback periods can be estimated as 14.4 to 15.4 years for Archimedes screws, 7.5 to 8.5 years for an overshot water wheel and 12 to 17 years for an undershot wheel, (with an expected lifetime of 30 years); these numbers are very low compared to Kaplan turbine installations with expected payback periods of 25 to 30 years (Müller and Kauppert, 2004). Water wheels can also be used in water distribution networks and systems (for example, irrigation networks), giving an additional value to the flowing water that is simultaneously used for power generation. The produced energy can be used to power the utilities of the water systems, thus reducing the greenhouse gas emissions (Menke et al., 2016).

1.1 Scope of the work

In Quaranta and Revelli (2015a), a theoretical model has been proposed to estimate the power losses of breastshot wheels. In Vidali et al. (2016), a dimensional approach was performed. In another study by Quaranta and Revelli (2016b), the number of blades has been investigated for breastshot water wheels. Concerning the blade profile, the general criteria that should be taken into account in the blade design are well established (Quaranta and Revelli, 2015a), whereas numerical or experimental investigations on the optimal profile of fast breastshot wheel blades can rarely be found. The general design criteria for the blade profile are listed in the following.

1. The relative entry stream velocity in the impact point should be directed at the blade inclination in order to reduce the inflow power losses.

2. The uplift of water downstream of the wheel and the outflow power losses should be minimized. Hence, the blades should exit at a normal angle with respect to the free surface at the tailrace or with a backward inclination in order to reduce the drag.

3. The blade length should be long enough or curved in order to avoid losses of water at the root of the blades.

Therefore, the aim of this paper is to investigate the effect of the blade profile on the performance of fast breastshot wheels with computational fluid dynamic (CFD) simulations. This is justified by the fact that, although the general criteria for the blade profile are well established, it is not so clear whether the blade profile generates significant effects on the performance of this kind of wheel (as previously illustrated). Similar uncertainty has also been found for Poncelet wheels: in Weisbach (1849) and Faibairn (1864), a circular shape is suggested, while Bresse (1869) concludes that the blade curvature is a matter of indifference. This work is also motivated by the need to improve the performance of an existing wheel by acting on the blade shape. The existing wheel with its original blade profile was simulated and then two different profiles were also investigated. The 1 : 2 physical scale model of this wheel with the original blade profile has also been installed in the hydraulics laboratory at the Politecnico di Torino, both to study the performance of breastshot wheels in detail (Quaranta and Revelli, 2015a) and to validate the numerical model. The detailed experimental results are reported in Quaranta and Revelli (2016).

CFD simulations for gravity water wheels have already been successfully conducted in Quaranta and Revelli (2016b); the performance of the present breastshot water wheel has been investigated through CFD simulations for

Figure 1. The existing breastshot water wheels, for which a 1 : 2 scale model was investigated in this work. The original diameter is 4 m.

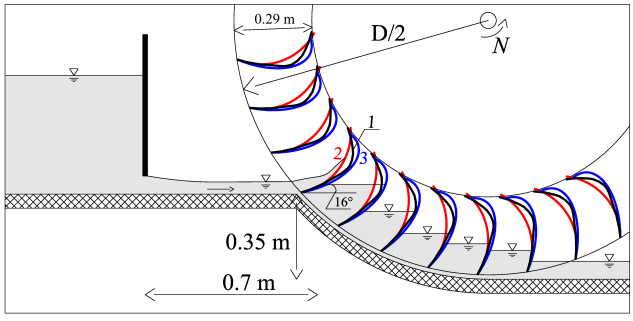

Figure 2. A sketch of the investigated breastshot water wheel with the three blade profiles investigated (profile 1 is the original profile), which is a 1 : 2 scale model of the existing water wheel.

different blade numbers. CFD simulations for stream water wheels have also been performed by Liu and Peymani (2012) and Akinyemi and Liu (2015).

2 Methods

The investigated breastshot water wheel is a 1 : 2 scale model (Froude similarity) of an existing wheel located in Verolengo, near Turin, Italy (Fig. 1); it is made up of 32 blades and the diameter is 4 m. The scaled wheel is 2.12 m in diameter and the width of the installed wheel is $b = 0.65$ m. The channel that conveys water to the wheel is 0.67 m wide; 0.7 m upstream of the entry point to the wheel there is a sluice gate. The geometric head (or channel drop, which is the difference between the elevation of the channel bed upstream and downstream of the wheel) is 0.35 m; thus, the wheel is a low breastshot wheel.

Furthermore, since the water flow accelerates by passing under the undershot weir (through the sluice gate opening), the blades are shaped so that, at the beginning of the filling process, the jet flows along them (before coming to rest in the buckets), and the inflow process is similar to Poncelet wheels. In Fig. 2 is a sketch of the scaled wheel.

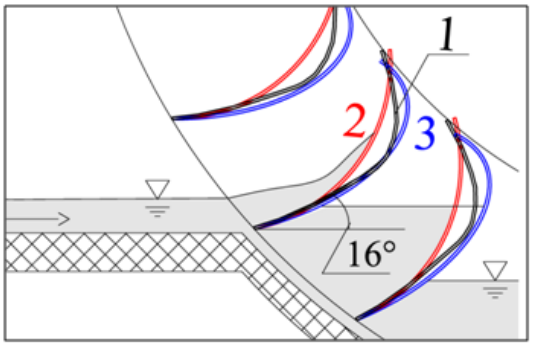

Figure 3. The zoom on the blades investigated in this work: (1) the original profile, (2) the circular profile and (3) the elliptical profile.

2.1 Blade profile

Three different shapes are investigated here through CFD analyses: the profile of the existing blades (1), a circular optimized modified profile (2) and an elliptical profile (3) (Fig. 3). The modified profiles (2) and (3) are designed with the same tip inclination of profile (1), which is 16° on the horizontal in the entry point, in order to objectively compare the effect of the different profiles. The tip inclination of the profiles is almost parallel to the relative flow velocity in order to minimize the impact power losses. In this case, the profiles also minimize the downstream power losses, since they exit from the tailrace approximately normally, without uplifting water. The angle between the profiles and the tailrace water surface is 83°; it is preferable for this to be smaller than 90°, since the slight backward inclination at the tip allows for a reduction in the drag. These profiles follow well-defined geometric shapes so that their fabrication process can be easily automated, also when water wheels are constructed by artisans, for example in rural areas and lower-income countries.

Profile (1) is 0.40 m long, and it can be considered as composed of three parts. The first part of the profile (which immediately starts to interact with the flow) is a circular arc 0.22 m long and 0.60 m in radius. This part of the profile seems to be quite flat. The third part (internal) is flat and 0.1 m long. The two previously described parts are connected by a circular arc 0.08 m long and 0.11 m in radius. The external part of the profile, which is the part that interacts mostly with the flow, is similar to the profile that would be obtained following the design procedure described in Weisbach (1849) for Poncelet wheels. In order to apply the design procedure described by Weisbach (1849) to the present wheel, the tip inclination of the blade in the impact point and the depth of the blades are required, which are 16° and 0.29 m, respectively; thus, the tip inclination on the horizontal is 62° under the wheel axis. The circular profile that would be obtained using the Weisbach procedure would have a radius of 0.62 m, which is very close to the real one in profile (1) of 0.60 m. However, in our case we do not deal with an original Poncelet water wheel because Poncelet wheels are generally installed

in straight channels with no geometric heads or channel bed drops through the wheel. Therefore, the radius of curvature of the procedure suggested by Weisbach (1849) for the blade design, which is similar to the existing profile, may not be optimal for this breastshot water wheel. Therefore, two different profiles were also investigated.

Profile (2) is a circular arc. A circular profile was studied to make the manufacturing process easier and because Weisbach (1849) and Faibairn (1864) also suggest a circular shape. The shorter the radius of curvature, the more deviation the jet, flowing along the blade, undergoes; this corresponds to a change in its momentum. The change in momentum leads to a force on the blade, pushing the wheel more than what would occur using a straight blade or a bigger radius of curvature. However, if the radius of curvature is too short, the jet may not be able to flow along the blade; it would separate from the blade surface, since at some points the profile direction may become vertical. Furthermore, the blade may uplift water from the tailrace, generating power losses. For example, in the present case considering the configuration of the entry point, a curvature radius of 0.2 m ($1/5\ R$, with R as the wheel radius) would result in a portion of the profile being vertical. This would generate a separation of flow and resistance; the flow would tend to decrease during the filling process, with power losses. Therefore, we considered a blade radius of $r = 1/4\ r = 0.25$ m, where $R = D/2$ is the wheel radius, as optimal.

Profile (3) is an elliptical shape: the major axis is again 0.25 m and the minor one is 0.14 m. This profile can also be considered good, since it exits at an optimal angle from the water surface of the tailrace, satisfying the points explained in Sect. 1.1.

2.2 Numerical model: geometry and mesh setup

The computational domain of the numerical model was divided into the stationary domain of the channel, which supplies water to the wheel, the rotating domain of the water wheel and the stationary air-filled domain outside the wheel. The stationary air domain is subdivided in an internal domain, directly in contact with the wheel, and an external domain (Fig. 4).

The channel and the wheel are meshed with 3-D tetrahedral elements. In order to check the mesh independence of the solution, the buckets were meshed with elements of 0.02 m and then with elements of 0.01 m near the blades. The stationary air domain is meshed with tetrahedral and cubic elements with a dimension of 0.02 m near the wheel and the channel and up to 0.1 m at the boundaries of the external domain. In order to save further time, half of the domain of the wheel (π rad instead of the whole 2π rad domain) was simulated with blades, while the other half of the wheel was simulated with a coarser mesh and without blades (Quaranta and Revelli, 2016b). The water wheel material was selected as steel, as in real cases.

2.3 Numerical model: simulation setup and boundary conditions

The flow field was modeled with the 3-D Reynolds-averaged Navier–Stockes (RANS) equations; the modeling was thus performed with one continuity and three momentum equations for the time-averaged pressure and velocity of the mixture (using commercial software). In order to solve these equations, the turbulent viscosity μ_t is introduced for modeling the Reynolds stresses. The turbulent viscosity μ_t was modeled using the shear-stress transport (SST) $k-\omega$ closure turbulent model, where the turbulent viscosity is expressed as a function of the turbulent kinetic energy k and the specific dissipation rate $\omega = \varepsilon/k$; ε is the turbulence kinetic energy dissipation. Hence, two additional equations are solved, one for k and the second for ω, determining the turbulent viscosity μ_t.

The volume of fluid (VOF) method was used for the multiphase problem, with an implicit interpolation scheme and a level set method, which is a well-established interface tracking method for dealing with two-phase flows with topologically complex interfaces. The turbulence damping option was included in the interface area to model such flows correctly; indeed, in free surface flows, a high-velocity gradient at the interface between two fluids may generate high turbulence, both in water and air. The curvature correction was also enabled to sensitize the model to the system rotation and streamline curvature.

The pressure–velocity coupling was solved with the PISO scheme and the spatial discretization was made with the PRESTO scheme for pressure and the second-order upwind scheme for momentum and turbulent kinetic energy. A modified high-resolution interface capturing (HRIC) scheme was used to compute the volume fraction. The mass flow rate was imposed at the channel inlet; also specified were the free surface level, the value of the turbulence intensity $I = 0.05$ and a fixed value of the turbulent viscosity ratio $\mu_t/\mu = 10$ with $\mu = 1 \times 10^{-3}$ as the water dynamic viscosity. The water density was set at $1000\,\mathrm{kg\,m^{-3}}$. At the outlet of the channel and at the external surfaces of the external air domain, the pressure outlet option was adopted. At the top of the external domain, the symmetry boundary condition was imposed (it gives more stability to the solution, with no effects on the interaction between the water and the wheel). Since the wheel is symmetrical with respect to a vertical plane perpendicular to the rotation axle, the symmetry boundary condition was imposed on this surface, and only half of the wheel was simulated, saving computational time. The no-slip boundary condition was imposed at the walls (the blade surfaces, canal walls and wheel), as shown in Fig. 4. The detailed numerical model is described in Quaranta and Revelli (2016b), in which the same water wheel has been investigated for different blade numbers.

The opening of the sluice gate was set at 0.075 m; flow rates of 0.05, 0.06 and $0.07\,\mathrm{m^3\,s^{-1}}$ were adopted and optimal

Table 1. The investigated working conditions and torque results.

Q ($m^3\ s^{-1}$)	N ($rad\ s^{-1}$)	C_{exp} (Nm)	$\hat{C}_1$ (Nm)	$\hat{C}_2$ (Nm)	$\hat{C}_3$ (Nm)	$\frac{\hat{C}_1 - C_{exp}}{\hat{C}_{exp}}$	$\frac{\hat{C}_2 - \hat{C}_1}{\hat{C}_1}$	$\frac{\hat{C}_3 - \hat{C}_1}{\hat{C}_1}$
0.05	0.78	175	173	180	170	−1.11 %	+4.0%	−1.7 %
0.06	0.79	223	211	226	205	−5.4 %	+7.1%	−2.8 %
0.07	0.89	253	239	244	219	−5.5 %	+2.1%	-8.4 %

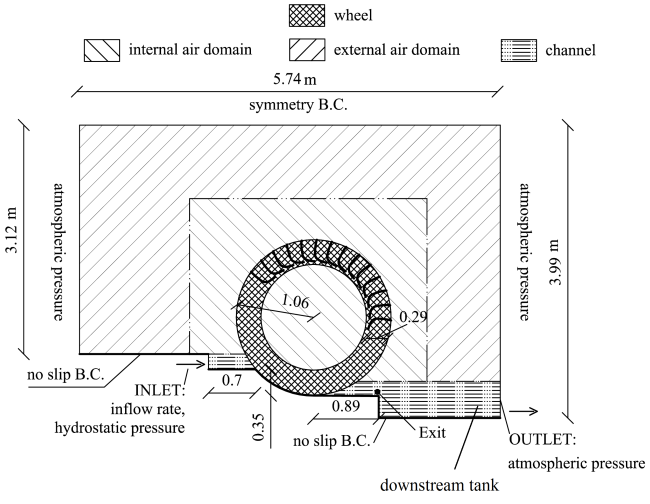

Figure 4. The numerical domain and the boundary conditions for the CFD model (Quaranta and Revelli, 2016b).

rotational speeds were chosen based on the experimental results described in Quaranta and Revelli (2015a) and Quaranta and Revelli (2016a), where the experiments are described in detail. Table 1 reports the investigated working conditions. In these cases, the downstream water depths were 0.07, 0.085 and 0.095 m, depending on the flow rate.

Once the numerical model with profile (1) was validated, it was possible to obtain a performance optimization by changing the shape of the blades in the geometry of the numerical model.

3 Results

The time step chosen for the unsteady simulation was 0.0008 s, which sometimes needed to be reduced to 0.0005 s. The second-order implicit scheme in time was used; 20 inner iterations were carried out between two consecutive time steps for the pressure–velocity solving. Each time step took approximately 2 min to be solved in a processor at 2.40 Ghz with 8 GB of RAM, for a total time of approximately 7 days for each simulation.

Since the shaft torque (exerted by the water on the blades of the wheel) could be easily monitored and represents a direct measurement of the water wheel performance, the torque was chosen as a control parameter for the simulations. During the simulations, the shaft torque C_j (with j as the blade profile) due to the water–blade interaction was monitored. When the blades began to interact with the stream, the torque started to increase. Due to the wheel radial symmetry, after the transitory time the torque trend oscillates periodically around the average value $\hat{C}_j$ with a period of $T = \beta/N$ (where β is $2\pi/n$, and n is the number of blades). The average value $\hat{C}_j$ was then compared with the experimentally measured value C_{exp} (with an accuracy of 6 Nm) to test the accuracy of the solution. Once the torque was calculated, the mechanical power output could be easily obtained by multiplying the torque by the rotational speed.

A mesh-sensitivity analysis and a validation on the torque and water depth was performed to check the mesh independence of the solution. This was discussed in Quaranta and Revelli (2016b), showing that both meshes are fine enough to capture the mean flow field and to calculate the wheel performance. The accuracy of the numerical model was determined by calculating the discrepancies between the numerical and the experimental solution using the finer mesh. The numerical model underestimates the torque, but the accuracy of the numerical shaft torque prediction is very good, with the average discrepancy between the numerical and experimental torques lower than 5 % (Table 1). At the flow rate of 0.05 $m^3\ s^{-1}$, the discrepancy is 1.11 %, while the discrepancy settles around 5.5 % for the higher flow rates; it is practically the same for discharges of 0.06 and 0.07 $m^3\ s^{-1}$.

Table 1 illustrates the performance of the wheel for different blade shapes, with respect to the original profile. As can be seen, the second profile is optimal, while the elliptical profile is the worst. The circular profile allows for a reduction in the power losses at the inflow, since the momentum of the flow is better exploited. It is also optimal for the downstream conditions, since a circular profile can exit the free surface at a better angle during its rotation. Table 1 also shows the percentage of increase in the two new profiles with respect to the real blade profile. The increase is between 2 and 7.1 % for the modified circular profile and between −1.7 and −8.4 % for the elliptical profile. For detailed information on the hydraulic behavior of the wheel, refer to Quaranta and Revelli (2016b). In conclusion, the achieved results show that the profile of the blades affects the performance of the wheel, and thus their curvature is not a matter of

indifference as expressed in Bresse (1869). In this case, the circular profile is preferable to the elliptical profile in order to increase the wheel efficiency.

4 Conclusions

Water wheels are an environmentally friendly and efficient technology for producing energy, but only a small amount of research has been done on their performance characteristics in the last century. Due to their several advantages over turbines, water wheels may constitute a suitable technology, especially in rural areas and lower-income countries.

In the present paper, a study of three blade shapes of a breastshot water wheel is reported in order to improve its performance. Numerical CFD analyses are performed to deal with the 3-D turbulent multiphase problem. The numerical results show that the blade profile affects the performance of the wheel; the circular profile is better than both the elliptical profile and the existing profile. With the circular profile, the performance of the wheel was improved by an average of 4 % with respect to the existing one.

Therefore, for a practical application of similar breastshot water wheels, the authors recommend using a circular profile, considering that the profile should be designed with the tip inclination parallel to the relative entry stream velocity; meanwhile, the blade should exit at an approximately normal angle from the tailrace. Simultaneously, the profile should be able to exploit the momentum of the water flow, while avoiding separation phenomena.

Data availability. The simulation data can not be made public for agreement reasons and file dimensions in term of GB. Please contact the authors.

Competing interests. The authors declare that they have no conflict of interest.

Acknowledgements. The research leading to these results has received funding from ORME (Energy optimization of traditional water wheels) – granted by Regione Piemonte via the ERDF 2007–2013 (grant number 0186000275) – partners Gatta srl, BCE srl, Rigamonti Ghisa srl, Promec Elettronica srl and Politecnico di Torino. We would also like to acknowledge the editor and the reviewers for their suggestions.

Edited by: E. Abraham
Reviewed by: two anonymous referees

References

Akinyemi, O. S. and Liu, Y.: CFD modeling and simulation of a hydropower system in generating clean electricity from water flow, International Journal of Energy and Environmental Engineering, 6, 357–366, doi:10.1007/s40095-015-0180-2, 2015.

Bozhinova, S., Kisliakov, D., Müller, G., Hecht, V., and Schneider, S.: Hydropower converters with head differences below 2.5 m, Proceedings of the ICE-Energy, 166, 107–119, 2013.

Bresse, M.: Hydraulic Motors, New York, J. Wiley and Sons, 1869.

Fairbairn, W.: Treatise on Mills and Millwork, Longman Green & Roberts, London, 1864.

Kallis, G. and David B.: The EU water framework directive: measures and implications, Water policy, 3.2, 125–142, 2001.

Laghari, J. A., Mokhlis, H., Bakar, A. H. A., and Mohammad, H.: A comprehensive overview of new designs in the hydraulic, electrical equipments and controllers of mini hydro power plants making it cost effective technology, Renewable and Sustainable Energy Reviews, 20, 279–293, 2013.

Liu, Y. and Peymani, Y.: Evaluation of paddle wheels in generating hydroelectric power, IMECE 2012-85121, IMECE 2012, Houston, TX, USA, 2012.

Menke, R., Abraham, E., Parpas, P., and Stoianov, I.: Demonstrating demand response from water distribution system through pump scheduling, Appl. Energ., 170, 377–387, 2016.

Müller, G. and Kauppert, K.: Old watermills – Britain's new source of energy?", Proceedings of the ICE-Civil Engineering, 12738, 178–186, 2002.

Müller, G. and Kauppert, K.: Performance characteristics of water wheels, J. Hydraul. Res., 42, 451–460, 2004.

Poncelet, J. V.: Memoria sulle ruote idrauliche a pale curve, mosse di sotto, seguita da sperienze sugli effetti meccanici di tali ruote, Translated by Errico Dombrè, Dalla tipografia Flautina, Napoli, 1843.

Quaranta, E.: Investigation and optimization of the performance of gravity water wheels, Doctoral dissertation, Politecnico di Torino, under review, 2017.

Quaranta, E. and Müller, G.: *Sagebien* and *Zuppinger* water wheels for very low head hydropower applications with head differences between 0.3 and 1.5 m, J. Hydraul. Res., under review, 2017.

Quaranta, E. and Revelli, R.: Performance characteristics, power losses and mechanical power estimation for a breastshot water wheel, Energy, 87, 315–325, 2015a.

Quaranta, E. and Revelli, R.: Output power and power losses estimation for an overshot water wheel, Renewable Energy, 83, 979–987, 2015b.

Quaranta, E. and Revelli R.: Optimization of breastshot water wheels performance using different inflow configurations, Renewable Energy, 97, 243–251, 2016a.

Quaranta, E. and Revelli, R.: Hydraulic behavior and performance of breastshot water wheels for different numbers of blades, Hydraulic Engineering, 143, 04016072, doi:10.1061/(ASCE)HY.1943-7900.0001229, 2016b.

Vidali, C., Fontan, S., Quaranta, E., Cavagnero, P., and Revelli, R.: Experimental and dimensional analysis of a breastshot water wheel, J. Hydraul. Res., 54, 473–479, 2016.

Weisbach, J.: Principles of the mechanics of machinery and engineering, Published by Lea and Blanchard, Philadelphia, 1849.